ELSEVIER

Magnetic Resonance Imaging 22 (2004) 815–825

MAGNETIC RESONANCE IMAGING

Application of spherical harmonics derived space rotation invariant indices to the analysis of multiple sclerosis lesions' geometry by MRI

Daniel Goldberg-Zimring[a,b,*], Anat Achiron[c], Simon K. Warfield[b], Charles R. G. Guttmann[d], Haim Azhari[a]

[a]*Department of Biomedical Engineering, Technion, Israel Institute of Technology, Haifa, Israel*
[b]*Computational Radiology Laboratory, Brigham and Women's Hospital and Harvard Medical School, Boston, MA, USA*
[c]*Multiple Sclerosis Center, Sheba Medical Center, Tel-Hashomer, Israel*
[d]*Center for Neurological Imaging, Brigham and Women's Hospital and Harvard Medical School, Boston, MA, USA*

Received 20 May 2003; accepted 27 January 2004

Abstract

In the longitudinal study of multiple sclerosis (MS) lesions, varying position of the patient inside the MRI scanner is one of the major sources of assessment errors. We propose to use analytical indices that are invariant to spatial orientation to describe the lesions, rather than focus on patient repositioning or image realignment. Studies were made on simulated lesions systematically rotated, from in vitro MS lesions scanned on different days, and from in vivo MS lesions from a patient that was scanned five times the same day with short intervals of time between scans. Each of the lesions' 3D surfaces was approximated using spherical harmonics, from which indices that are invariant to space rotation were derived. From these indices, an accurate and highly reproducible volume estimate can be derived, which is superior to the common approach of 2D slice stacking. The results indicate that the suggested approach is useful in reducing part of the errors that affect the analysis of changes of MS lesions during follow-up studies. In conclusion, our proposed method circumvents the need for precise patient repositioning and can be advantageous in MRI longitudinal studies of MS patients.

Keywords: Multiple sclerosis; 3D geometry; Spherical harmonics; Repositioning errors; Longitudinal study; Shape change

1. Introduction

In the study of multiple sclerosis (MS), and especially during longitudinal studies of patients using magnetic resonance imaging (MRI), an accurate assessment of the lesion load is of utmost importance. Incorrect repositioning of the patient inside the MRI scanner is one of the major sources of assessment errors and is considered as "inevitable," even with the application of repositioning techniques [1]. In MS, because the lesions are usually small compared to typical voxel resolution, a slight change in position can cause notable changes in lesions' size and shape [1–3]. In order to minimize the effects of an inaccurate repositioning, different approaches have been applied. These include mechanical methods such as masks that hold the patients' head static, light markers, MRI markers, and reference set of images [4,5]. The improvement of spatial resolution during image acquisition and the acquisition of images in a contiguous fashion [1] were also proposed to reduce the repositioning error. Filippi et al. [6] studied the effects of an imprecise repositioning by combining several repositioning methods such as landmarks, a light indicator, T_1-weighted reference scans, and head immobilization shells. They reported variations in the range of 1.4% to 6.8% in volume estimation, even with the implementation of these techniques.

Postacquisition image registration algorithms had also been developed in an effort to even further minimize the repositioning errors [2,3]. Hajnal et al. [3] found that even with the use of the mechanical or image acquisition methods, the positional match between image sets was usually no better than 1–2 voxels (typically 1–2 mm). They improved this positional match by developing a rigid body translation and rotation algorithm that uses sinc interpolation and a least square optimization procedure, with which they achieved an alignment of images to a fraction of a voxel

* Corresponding author. Tel.: +1-617-525-6229; fax: +1-617-525-6220.
E-mail address: daniel@bwh.harvard.edu (D. Goldberg-Zimring).

0730-725X/04/$ – see front matter
doi:10.1016/j.mri.2004.01.053

(typically < 0.01 mm in each linear dimension). Guttmann et al. [7] analyzed the variability in MS lesion volume measurement. They acquired the brain MR images within short intervals of time between two imaging sessions for which the patients exited and re-entered the scanner room. At each time the patient's head was positioned in a neutral position. Two radiology technologists alternated in positioning the patient, to minimize bias. Foam pads and tape were the sole devices used to stabilize the head within the standard head-holder in the quadrature head coil. Additionally, they applied a multi-step postacquisition processing to the images that included the segmentation of the intracranial cavity, the use of an anisotropic diffusion filter, partial volume correction, an automatic image registration, and fully automated image segmentation. Their results showed an average lesion volume difference between two MR exams of the same patient of 0.05 cm^3.

Spherical harmonics (SH) are used to quantitatively define and calculate different three-dimensional (3D) geometrical features [8], including the surfaces of MS lesions [9]. The geometry of the studied lesion can be characterized by indices, which are invariant to spatial orientation. In the present study, we used simulated, in vitro, and in vivo MS lesions for analyzing the utilization of SH-derived space rotation invariant indices and volumes derived from them, as an analytical method to overcome or reduce the effects caused by an imprecise repositioning of MS patients inside the MRI scanner.

2. Methods

2.1. Spherical harmonics

Spherical Harmonics (SH) are orthonormal functions over the unit sphere utilized to describe complicated surfaces in 3D. These functions are defined by [10]:

$$Y_{lm}(\theta,\varphi) = \sqrt{\frac{2l+1}{4\pi}\frac{(l-m)!}{(l+m)!}}P_l^m(\cos\theta)\exp(im\varphi) \tag{1}$$

where $Y_{lm}(\theta,\varphi)$ is the corresponding SH function defined in a spherical coordinate system (R,θ,φ), $P_l^m(\cos\theta)$ is the associated Legendre polynomial, the parameter l (function's degree) is zero or a positive integer and the integer m (function's order) can have only the values of $-l$, $-(l-1)$ $\ldots$, 0, $\ldots$, $(l-1)$, l.

For a spherical coordinate system (i.e., R,θ,φ), the surface radii R can be discretely presented by:

$$R(\theta,\varphi) = \sum_{l=0}^{\infty}\sum_{m=-l}^{l} r_{lm}Y_{lm}(\theta,\varphi) \tag{2}$$

where r_{lm} are the amplitudes of the corresponding SH functions (represented by complex numbers). Equation (2) can be represented as a multiple linear regression model. Thus, by using a least squares approximation, a MS lesion can be analytically described by calculating the corresponding r_{lm} coefficients [9].

2.2. Characterization of lesion geometry using spherical harmonics

The entire procedure for the lesion geometry characterization, as well as an extended comparison for lesion volume calculation, including partial volume effects between our method and the commonly used technique that multiplies the lesions' 2D contours' areas by slice thickness (referred to herein as a "cylindrical approximation" [CA]), was done and explained in detail in [9]. In summary, sets of contours for each individual MS lesion taken from segmented MR images are used to approximate the lesions' 3D geometry. As the density of samples on the contour was not always equal, in order to obtain the same number of points in all traced contours, each of the contour lines was interpolated and resampled. Later, the points of each contour were rearranged in such a way that the first point was the most extreme point on the right-hand side in each contour. The rest of the points were then registered in a counterclockwise direction. As only axial slices were acquired here, in order to constrain the SH expansion along the direction perpendicular to the axial plane, a sagittal and a coronal contour were added by applying the Akima interpolation, a smooth curve fitting method [11]. The final sets of contours obtained for each lesion were then arranged according to their respective spatial orientation, yielding a 3D cluster of data points. Using this cluster of data points, the corresponding SH polynomial representation of the individual lesion is estimated and its 3D surface is reconstructed. The reconstructed surface was then virtually sliced into a high number of discrete slices and the lesion volume was calculated by summing the corresponding areas of all discrete slices multiplied by its new discrete slice thickness.

In order to analyze the changes in the SH coefficients, each lesion has to be approximated using the same number of harmonics (n) at every position in the 3D space. In our previous study [9] we observed that the choice of n must be set according to the ratio of the lesion size to image resolution in order to avoid distortions in the estimated 3D surface. In the current study, due to the rotation of the lesions and the different positioning into the scanner, the number of contours obtained for each position varied. Therefore, n was chosen to be equal to the minimal number of axial slices in which the lesion extended for all positions. The effect of lesion size on the accuracy of the measurement was determined in [9]. There, we showed an average volume estimation error smaller than that obtained by the CA method, particularly when the lesions extended into 2–3 axial slices (the most common case in MS when using a 3-mm slice thickness).

The polynomial coefficients that describe the estimated

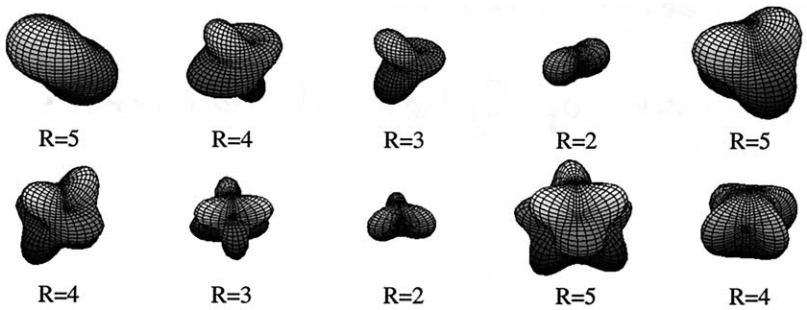

Fig. 1. Baseline views of the irregular shapes used for the simulations, with R their respective radii.

surfaces were then used to analyze the changes in the estimated MS lesions' size/volume and the changes in individual lesion shape. For the analysis, a space rotation invariant set of indices "I_l" was estimated using:

$$I_l = \sum_{m=-l}^{l} |r_{lm}|^2 \tag{3}$$

where $l = 0,1,2, \ldots,$ n. The obtained I_l indices were then normalized to the value of I_0 of the baseline position (i.e., $I_l/|r_{00}|^2$). The index I_0 comprises only r_{00}, which is the general average radius of the approximated surface. Thus, $I_0^{(1/2)}$ is proportional to the average radius of the shape and $I_0^{(3/2)}$ is proportional to the volume defined by the average radius. Thus, the variations in I_0 characterize the changes in the size/volume. The estimation of lesion volume by I_0 differs from the method for volume estimation done in [9] mainly because of the space rotation invariant property of I_0. Unlike I_0, which express global changes, the $I_{l>0}$ indices express morphological changes in the 3D SH shape. As l increases, the I_l indices correspond to finer and more localized changes in the lesion's surface. All the software used in the present study was homemade software written in Matlab 6.0 (Mathworks, Inc., Natick, MA, USA).

2.3. Simulated lesions

Simulated lesions were utilized to analyze the application of SH-derived space rotation invariant indices in the measurement of MS lesions' 3D geometry. Ten different simulated lesions representing irregular shapes were randomly constructed using SH. The distribution of the size of the lesions was according to the most frequent cases found in real lesions: three lesions had a radius of 5 voxels, another group of three lesions had a radius of 4 voxels, two had a radius of 3 voxels, and the last two lesions had a radius of 2 voxels. Most of the irregular shapes represent typical MS lesions or even more complicated shapes than the common ellipsoidal lesion geometry, thus making the analysis more complicated. Figure 1 presents the baseline views of the irregular shapes used for the simulations. The simulated lesion's surface points x, y, and z were rotated by using the following transformation matrix:

$$\begin{pmatrix} x' \\ y' \\ z' \end{pmatrix} = \begin{pmatrix} \cos\alpha, & -\sin\beta \cdot \sin\alpha, & \cos\beta \cdot \sin\alpha \\ 0, & \cos\beta, & \sin\beta \\ -\sin\alpha, & -\sin\beta \cdot \cos\alpha, & \cos\beta \cdot \cos\alpha \end{pmatrix} \cdot \begin{pmatrix} x \\ y \\ z \end{pmatrix} \tag{4}$$

where x', y', and z' are the rotated surface points, α is the rotation along the y-axis, and β the rotation along the x-axis. Each of the simulated lesions was rotated systematically along the x- and y-axes by combining 5 different angle values for α and β ranging from 0–11.25°, yielding 15 different positions, thus making a total of 150 analyzed virtual lesions.

Two different data sets were generated from these virtual lesions in each position: (I) By taking a discrete sampling of the 3D surface points. (II) By "virtual MR" imaging the lesions. This was done by assuming that the resolution was 1 pixel = 1 mm, and by slicing the lesions at every 3 pixels or every 2 pixels along the axial plane, yielding a 3-mm and a 2-mm slice thickness without gap, respectively. Synthetic MR images were generated by integrating all datapoints contained within the selected slice position (i.e., ± 1/2 slice thickness). As each of the synthetic images presented only one of the simulated lesions' 2D segments, the regions of interest were defined by values higher than 0 surrounded by 0s in the background. Therefore, lesions were segmented by applying thresholding, yielding a 2D contour for each lesion slice.

2.4. In vitro data

Imaging data was obtained from three in vitro half brains of patients who suffered from MS. The in vitro brains were obtained form the National Neurological Research Specimen Bank, The Multiple Sclerosis Human Neurospecimen Bank, Los Angeles, CA, USA. Each of the half brains was scanned twice on different days without making any effort in achieving precise repositioning. MR images were ac-

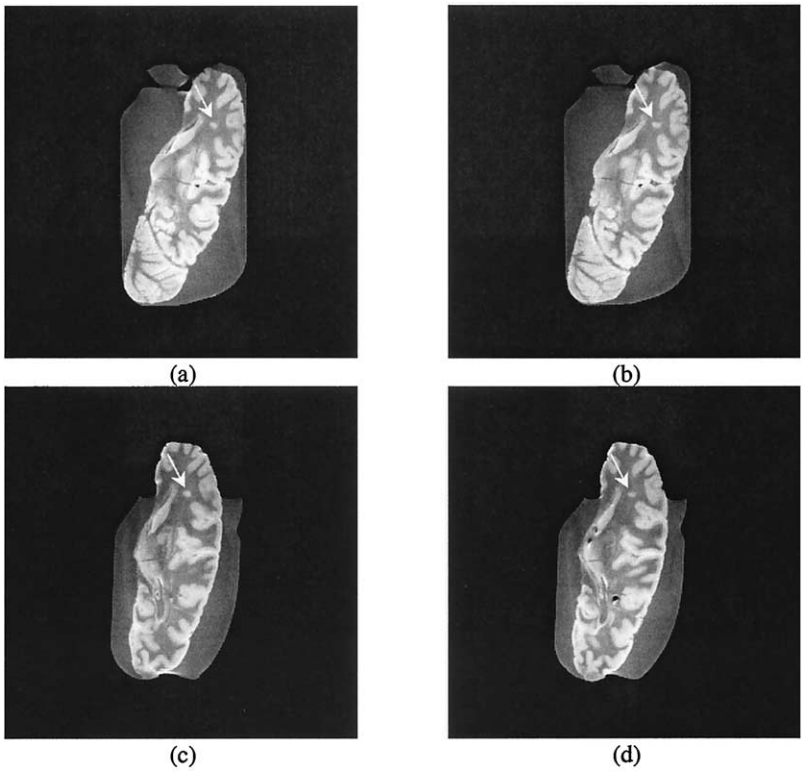

Fig. 2. (a,b) MRI slices of the first scan of the in vitro half brain into which the analyzed lesion (white arrow) was extended. (c,d) The same lesion in the MRI slices obtained by scanning the in vitro half brain on a different day without making any effort in achieving precise repositioning.

quired on a 2-T Elscint Prestige scanner (Elscint, Israel). As the brains were preserved in formalin, the best images were obtained with a T_1-weighted protocol (repetition time (TR)/echo time (TE) = 550/20, 24 cm field-of-view (FOV), and a 256 × 256 matrix). MS lesions presented a high-intensity signal contrasting with the low-intensity signal of the surrounding white matter. Images were acquired in the axial plane, 2-mm slice thickness (the best possible resolution using this scanner), and no gap. Figure 2a, b presents the MRI slices from the first scan of the in vitro half brain showing an analyzed lesion (white arrow), and Fig. 2c, d presents the same lesion (white arrow) in the MRI slices obtained on a different day. As can be noted, no attempt was made to align the half brains between scans. MS lesion contours were extracted by segmenting the observed lesions using an adaptive threshold algorithm [12].

2.5. In vivo data

Imaging data was obtained from a MS patient who was scanned five times the same day with short intervals of time between the scans. No effort was made to achieve an accurate repositioning of the patient inside the scanner. MR images were acquired on a 1.5-T Signa System (GE Medical Systems, Milwaukee, WI, USA). T_2-weighted images were obtained (TR/TE = 3000/30, 24 cm FOV, and a 256 × 256 matrix). Images were acquired in the axial plane 3-mm slice thickness, and no gap. Figure 3a–e, presents a MRI slice belonging to each one of the five sets of images, respectively. These images show one of the analyzed MS lesions (white arrow) that extended into 3 consecutive slices in all the scans. Because no repositioning technique was applied, differences between the images and the 2D shape of the lesion can be observed. Manual segmentation using mouse tracking was applied to extract the MS lesion's contours.

2.6. Analysis of the changes in the lesions' 3D shape

In the present study, we calculated and utilized the mean discrete total variation (MDTV) to estimate the mean amplitude of the oscillations for the changes in the normalized I_l indices. The discrete total variation is used to measure the total amplitude of discrete signal oscillations [13]. It is calculated by approximating the signal derivative by a finite difference over the sampling distance. The MDTV is given by:

$$MDTV_l = \frac{\sum_{t=1}^{N} |I_l(t) - I_l(t+1)|}{N} \quad (5)$$

where t is the position index and N is the total number of positions. The MDTV does not vary linearly with respect to changes in lesion size/volume.

The MDTV was first calculated for the changes in I_0. As a mean of comparison, the MDTV was also calculated for the lesions' volumes obtained using the CA method. Addi-

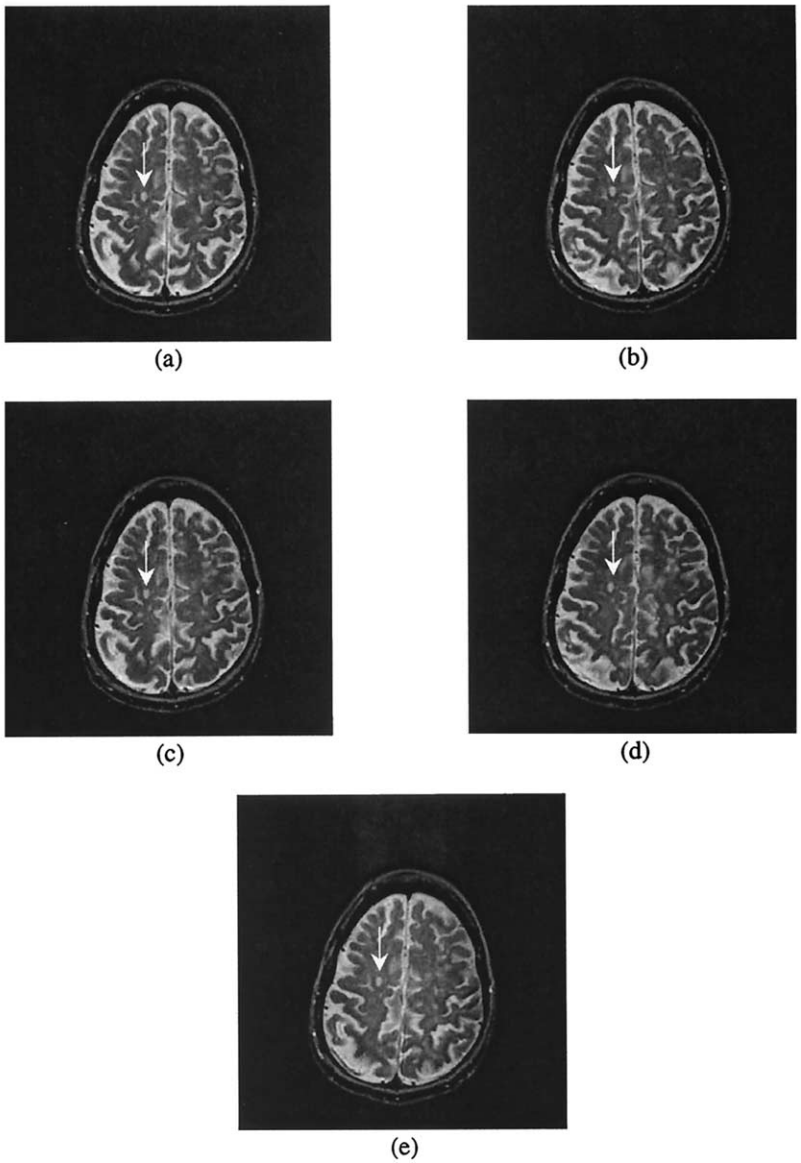

Fig. 3. (a–e) An in vivo MRI slice belonging to each one of the five sets of images, respectively, showing one of the analyzed MS lesions (white arrow). The differences between the images and the 2D shape of the lesion can be noted.

tionally, the coefficient of variation (COV) of the I_l indices was calculated by [14]:

$$COV = \frac{\text{Standard Deviation } (I_l)}{\text{Mean } (I_l)} \tag{6}$$

The MDTV and the COV were applied for analyzing the changes in lesions' shape expressed by each of the $I_{l>0}$ indices.

3. Results

3.1. Simulated lesions

The simulated lesions were first approximated using the discrete sampling points (data set I above). As expected, because of the space rotation invariance property of the I_l indices, in all the simulations the estimated MDTV and COV for I_l were exactly zero! As an example, Fig. 4 depicts the simulated MS lesion number 5 in 2 of the 15 different positions in which it was analyzed. The orthogonal axes were added to provide a better visualization of the rotation. For this simulated lesion, in all the positions, the normalized I_l indices were: $I_0 = 1$, and $I_3 = 0.13$ (because this particular simulated lesion was constructed using n = 3, all other indices equaled zero), yielding an average MDTV (AMDTV) and an average COV (ACOV) equal to zero.

Once the space rotation invariance property of the I_l indices was validated, the effect caused by imaging the simulated MS lesions as in a MRI process on the I_l indices was first analyzed for I_0 and then for $I_{l>0}$ (using data set II

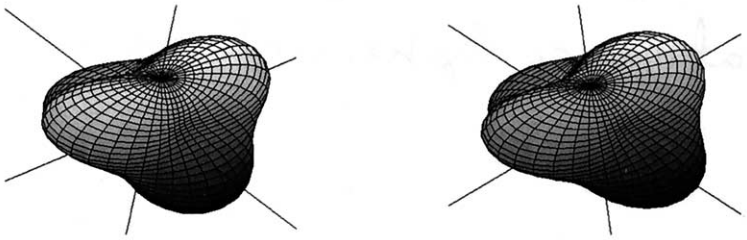

Fig. 4. Simulated MS lesion number 5 in 2 of the 15 different positions in which it was analyzed. The orthogonal axes were added to provide a better visualization of the orientation. For this simulated lesion, in all the positions, the normalized I_l indices were: $I_0 = 1$, and $I_3 = 0.13$ (since this particular simulated lesion was constructed using $n = 3$, all other indices equaled zero), yielding an $AMDTV = 0$ and an $ACOV = 0$.

above). The reconstruction of the simulated lesions' 3D shape was therefore obtained using the axial contours obtained from the "imaged" lesions. "Imaging" was first done with a 3-mm slice thickness and then followed by a 2-mm slice thickness with no gap between slices. According to the size of the simulated lesions, for the 3-mm simulation, two of the lesions were approximated using n = 2, five lesions were approximated using n = 3, and a value of n = 4 was used to approximate the remaining three lesions, therefore l varied from 1–4. For the 2-mm simulation two lesions were approximated using n = 2, one using n = 3, a value of n = 4 was used for three lesions, n = 5 for two other lesions, and the remaining two lesions using n = 6. The AMDTV and the ACOV were estimated for I_0 and compared with the AMDTV and the ACOV for the lesions' volumes estimated by the CA method for both cases. The results are outlined in Table 1. In Table 1, as well as in all subsequent tables, a zero value for the AMDTV and ACOV is expected when no changes are detected in the reconstructed 3D surfaces.

In order to verify that the differences between the obtained AMDTV and ACOV for I_0 were statistically significant from those obtained for the CA, a paired t test with a confidence level of 5% was done. For both cases, i.e., the 3-mm and 2-mm slice thickness, the statistical differences between the groups were significant ($p < 0.02$). This indicates that I_0 and corresponding volumes derived from it is less affected by inaccurate repositioning.

For the $I_{l>0}$ indices, l varied from 1 to 4 for the 3-mm slice thickness simulations and from 1 to 6 for the 2-mm slice thickness simulations, because the maximum number of harmonics used to approximate the lesions were 4 and 6, respectively. The estimated AMDTV and ACOV for I_1–I_5 are outlined in Table 2 (the number of measurements done for each index (N) are presented in the table, I_6 was omitted because only two measurements were available). For both cases, i.e., the 3-mm and the 2-mm slice thickness, the estimated AMDTV values were substantially lower than the values obtained for the ACOV. The difference between the obtained AMDTV and ACOV values stems from the fact that the local changes on the 3D surfaces are not well characterized by a Gaussian process but rather a more complicated nonstationary stochastic process. Therefore, we prefer the MDTV index to analyze local geometrical changes on the lesions' 3D surfaces.

3.2. In vitro data

Five MS lesions were identified in the MR images of the in vitro half brains and analyzed. Each lesion was segmented from the two sets of images acquired for each in vitro brain and approximated using SH. Because only two scans were available for each lesion, the AMDTV represents in this case only the average difference between the two measurements. (The ACOV is of course irrelevant here). The AMDTV values were estimated for I_0 and compared with the AMDTV estimated for the lesions' volumes by the CA method. The results are outlined in Table 3.

The normalized $I_{l>0}$ indices were also estimated for the in vitro lesions. According to the size of the identified lesions, two of the lesions were approximated using n = 2, three lesions were approximated using n = 3, and a value of n = 4 was used to approximate the fifth lesion, therefore l

Table 1
The estimated AMDTV and ACOV for I_0 and CA for the simulated lesions "imaged" with a 3-mm and a 2-mm slice thickness

	Simulated lesions (%)					
	3-mm slice thickness			2-mm slice thickness		
	N	*AMDTV*	*ACOV*	*N*	*AMDTV*	*ACOV*
I_0	10	1.5 ± 1.0 (0.5–3.2)	1.9 ± 1.0 (0.6–3.6)	10	1.4 ± 0.8 (0.6–3.0)	1.7 ± 0.9 (0.7–3.1)
CA	10	1.9 ± 1.0 (0.6–3.5)	2.8 ± 1.2 (1.1–4.5)	10	2.0 ± 0.9 (0.8–3.4)	2.3 ± 1.0 (0.9–4.1)

The numbers are represented as average mean discrete total variation (AMDTV) and average coefficient of variation (ACOV) ± standard deviation, with range in parentheses; N represents the number of measurements done for each index.

Table 2
The estimated AMDTV and ACOV for I_1–I_5 for the simulated lesions "imaged" with a 3-mm and a 2-mm slice thickness

	Simulated lesions (%)					
	3-mm slice thickness			2-mm slice thickness		
	N	*AMDTV*	*ACOV*	*N*	*AMDTV*	*ACOV*
I_1	10	0.5 ± 0.4 (0.1–1.4)	34.0 ± 23.3 (13.9–81.6)	10	0.5 ± 0.3 (0.1–1.0)	30.4 ± 11.2 (11.3–54.5)
I_2	10	0.8 ± 0.8 (0.2–2.8)	21.3 ± 16.3 (6.0–49.7)	10	1.0 ± 0.9 (0.2–2.8)	27.1 ± 16.1 (7.0–47.8)
I_3	8	1.0 ± 1.0 (0.1–3.0)	29.0 ± 18.8 (4.4–67.7)	8	0.5 ± 0.4 (0.1–1.3)	24.9 ± 11.0 (5.5–39.8)
I_4	4	0.4 ± 0.3 (0.2–0.8)	21.5 ± 8.2 (10.1–27.7)	8	0.5 ± 0.4 (0.1–1.4)	22.9 ± 13.9 (6.9–42.3)
I_5		-	-	4	0.2 ± 0.1 (0.1–1.3)	14.2 ± 6.6 (7.9–23.8)

The numbers are represented as AMDTV (average mean discrete total variation) and ACOV (average coefficient of variation) ± standard deviation, with range in parentheses; N represents the number of measurements done for each index.

varied from 1–4. The AMDTV were in the range of a few percents. The results for the estimated AMDTV for I_1–I_3 are outlined in Table 4 (I_4 was omitted because only one value was available). The reconstructed in vitro lesion shown in Fig. 2a,b and in Fig. 2c,d are depicted in Fig. 5a and b, respectively. The similarity between both approximations, showing principally the change in the lesion's spatial orientation, can be noted.

3.3. In vivo data

Eight MS lesions were identified in the MR images of the scanned patient. Each lesion was segmented from the five sets of acquired images and were approximated using SH. The AMDTV values were again estimated for I_0 and compared with the AMDTV estimated for the lesions' volumes by the CA method. The results are outlined in Table 5.

The normalized $I_{l>0}$ indices were then estimated for the in vivo lesions. In the analyzed sets of images, all the identified lesions were relatively small; they were extended into 2–3 contiguous axial slices (as pointed out above, the most common cases in MS lesions for a 3-mm slice thickness). According to the size of the identified lesions, five of the lesions were approximated using n = 2, and the other three lesions with n = 3, therefore l varied from 1–3. The results for the estimated AMDTV for I_1–I_3 are outlined in Table 6. The reconstructed in vivo lesion shown in Fig. 3a–e is depicted in Fig. 6a–e, respectively.

A paired t test with a confidence level of 5% was also applied to verify if the differences between the obtained AMDTV for I_0 were statistically significant from those obtained for the CA. From this statistical analysis, a $p < 0.03$ was obtained, indicating that the difference between the groups is significant, i.e., for the in vivo lesions I_0 was also less affected by inaccurate repositioning.

4. Discussion

The repositioning of patients inside the MRI scanner is a significant limitation of longitudinal studies of patients with MS by utilizing MR images. The variations due to an inadequate repositioning are sometimes overwhelming the changes caused by the disease. Different studies had investigated the effects of changes in head positioning inside the MRI scanner on MS lesion measurements. Barkhof et al. [1] reported that less than a 2° change in head repositioning can lead to "apparent" changes in lesion size. Hajnal et al. [3] pointed out that a change of 1° in the head position can produce a differential displacement of 2 mm across the brain, whereas Firbank et al. [15] found that a repositioning error of 1 mm could lead to differences in volume measurements of up to 12%, or a 30% difference in measured volume between two scans when a 5-mm slice thickness is used. Stone et al. [5] found that an imprecise repositioning causes about 4% of the 15% of the month-to-month fluctuations in measurement error. Similarly, Filippi et al. [6] found a mean absolute difference between two corresponding scans ranging from 1.4% to 6.8%. Gawne-Cain et al.

Table 3
The estimated AMDTV for I_0 and CA for the in vitro lesions

	In vitro MS lesions (%)	
	N	*AMDTV*
I_0	5	3.6 ± 2.5 (0.7–7.4)
CA	5	4.2 ± 3.5 (0.6–9.9)

The numbers are represented as AMDTV (average mean discrete total variation) ± standard deviation, with range in parentheses; N represents the number of measurements done for each index.

Table 4
The estimated AMDTV for I_1–I_3 for the in vitro lesions

	In vitro MS lesions (%)	
	N	*AMDTV*
I_1	5	1.0 ± 1.0 (0.1–2.3)
I_2	5	3.7 ± 3.9 (0.5–8.9)
I_3	3	5.1 ± 4.6 (1.4–10.2)

The numbers are represented as AMDTV (average mean discrete total variation) ± standard deviation, with range in parentheses; N represents the number of measurements done for each index.

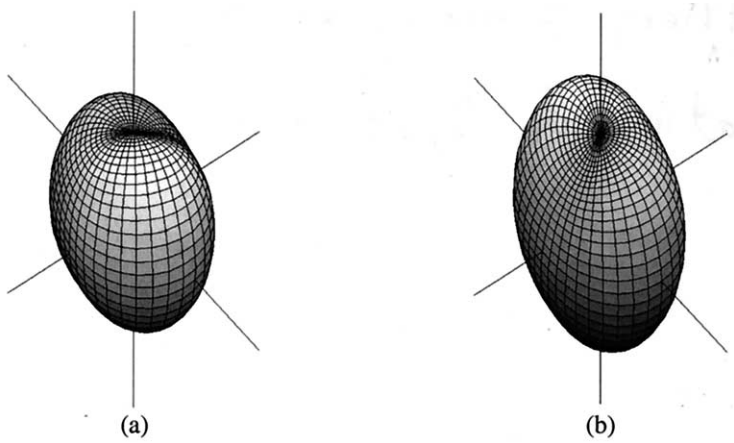

Fig. 5. (a) The reconstructed in vitro lesion shown in Fig. 2 a,b. (b) The reconstructed in vitro lesion shown in Fig. 2 c,d. The similarity between the reconstructed lesions, which are only affected by their respective 3D space orientation, can be noted. The orthogonal axes were added to provide a better visualization of the orientation.

[16] scanned five patients 10 times each, allowing a displacement from baseline of ± 4 degrees for an anteroposterial rotation and 3 mm of slice offset. They found that the worst-case difference between volumes in the same patient ranged from 8.9% to 32%, with the maximum potential error due to repositioning inaccuracies of a similar magnitude to the 5–10% expected change in lesion volume over 1 year. Most recently, Rovaris et al. [14] measured lesion load for repeated brain MRI after repositioning the patients following the ad hoc European Communities Committee guideline. Then, an experienced observer classified the sets of images into poor and good repositioning by visual judgment. A good repositioning was considered when the same anatomical structures were present either on the same slice or on ± 1 slice. They found a COV of 7.7% for the poor repositioned set of images (5 out of 9 sets) and an even higher COV of 10.0% for the 4 sets considered to have a good repositioning. For the total lesion load on the whole set of scans, a COV of 8.9% was found, which was higher than the 4.9% for the intraobserver reproducibility. Guttmann et al. [7] found an average lesion volume difference between two MR exams of the same MS patient of 0.05 cm^3, with a 95% confidence interval between −0.17 and 0.28 cm^3. They also found that the limits of agreement for lesion volume were between −1.3 and 1.5 cm^3, implying that in individual patients changes in lesion load need to be at least this large to be detected reliably.

In the present study, a totally different approach is presented. Use of analytical indices that are invariant to spatial orientation is suggested as an alternative or complementary technique for patient repositioning or image realignment.

The results obtained here for the simulated lesions rotated in the 3D space, and for the in vitro MS lesions scanned twice without making any effort for achieving precise repositioning, show that the effects of an imprecise repositioning on the analysis of changes done using I_0 are significantly lower than those for the volume estimated by the CA method. For the analysis of the shape changes (i.e., for $I_{I>0}$), the differences between the AMDTV and the ACOV were clearly significant, thus it can be concluded that the COV is not an indicative parameter for analyzing morphological changes.

Although the normalized I_I indices were effectively invariant to a spatial rotation for the simulated lesions that were approximated using a discrete sampling of their surfaces, for the "imaged" simulated lesions, the normalized I_I indices presented variations yielding an AMDTV and an ACOV greater than zero. The statistical analysis done for the "imaged" lesions showed significant differences between the index I_0, which represents the changes in the lesions' size, and the changes in the volumes estimated by the CA method. As observed, the effects of an imprecise repositioning on the analysis of changes done using the I_0

Table 5
The estimated AMDTV for I_0 and CA for the in vivo lesions

	In vivo MS lesions (%)	
	N	*AMDTV*
I_0	8	7.1 ± 2.8 (3.2–10.6)
CA	8	9.9 ± 5.7 (3.7–17.2)

The numbers are represented as AMDTV (average mean discrete total variation) ± standard deviation, with range in parentheses; N represents the number of measurements done for each index.

Table 6
The estimated AMDTV for I_1–I_3 for the in vivo lesions

	In vivo MS lesions (%)	
	N	*AMDTV*
I_1	8	2.6 ± 2.9 (0.2–8.7)
I_2	8	7.9 ± 3.6 (3.5–13.6)
I_3	3	3.5 ± 2.5 (1.0–6.0)

The numbers are represented as AMDTV (average mean discrete total variation) ± standard deviation, with range in parentheses; N represents the number of measurements done for each index.

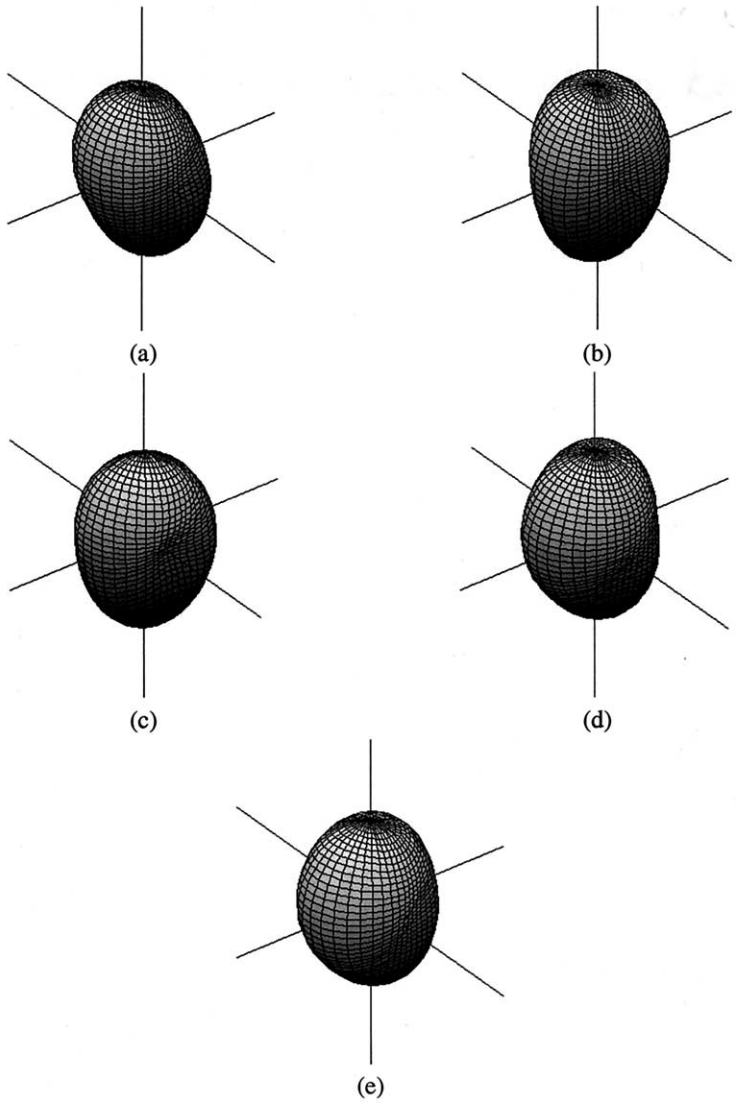

Fig. 6. The respective reconstructed in vivo lesion shown in Fig. 3 a–e. A close similarity between the reconstructed lesions, which are mainly affected by their respective 3D space orientation, can be noted. The orthogonal axes were added to provide a better visualization of the orientation.

index are significantly lower than those for the CA method. For the analysis of morphological changes (i.e., for $I_{l>0}$), the differences between the AMDTV and the ACOV were clearly significant, thus it can be concluded that the COV is not an indicative parameter for analyzing changes in lesions' shapes.

For the in vitro MS lesions, the obtained results for the AMDTV values were relatively higher than those obtained for the simulated lesions. The difference can be attributed to the fact that all the simulations were not affected by image acquisition noise caused by the MRI scanner itself, e.g., magnetic field inhomogeneities, radiofrequency noise, etc. Other sources of error such as motion, pulsatility, and blood flow are not included in the in vitro images, however the in vitro brains were used as the most realistic available MS phantom. As previously pointed out by others, it is known that no phantom is able to reproduce satisfactorily the complexity of MS lesions and white matter in composition, relaxation characteristics, shape, and spatial distribution (see, e.g., [7]).

For the in vivo MS lesions, the above-mentioned sources of noise in the images made the analysis more complicated and the obtained *AMDTV* values were even higher. However, the results are within the range of the results presented in the literature when mechanical methods for achieving good repositioning of the patients inside the scanner were applied [6,14,16]. The statistical analysis done for the in vivo lesions also showed significant differences between the index I_0 and the changes in the lesions' volumes estimated by the CA method. While acknowledging that because of the interpatient MS lesion variability a more extensive study is needed in which lesions taken from different patients will be analyzed, our study takes into account the also-known intrapatient lesion variability.

In the present study we used conventional dual-echo MR images, with a through-plane resolution of 2 mm and 3 mm.

By acknowledging that if the acquisition of the MR images is done using a better resolution (e.g., 1-mm isotropic sampling) it might be possible to use a higher n value and achieve better approximation for irregular MS lesions. On the other hand, thinner slice volume frequently decreases signal to noise ration (SNR) and lesion contrast, thus it may trade off lesion delineation for spatial resolution, which is particularly true for the MS lesions. However, it should also be noted that newer imaging techniques such as Single Slab 3D fast spin echo [17] allow the acquisition of higher isotropic resolution (e.g., 1 mm^3) T_2-weighted images with adequate SNR. This technique has only recently started to be applied to the analysis of MS lesions. Additionally, other modern MRI techniques such as 3D fast spin echo, magnetization transfer, and diffusion tensor MR images are also currently being used to investigate the pathophysiology of MS and could eventually help reduce measurement errors. It can be expected that the combination of such new image acquisition techniques together with the method suggested here would improve the analysis of changes in even smaller MS lesions. A more accurate total lesion load could be estimated by adding the individual lesion volumes that are more accurately obtained using the suggested method.

The immediate question that emerges here is how sensitive is the method proposed in the present work to analyze the real changes in MS lesions' size and shape. This question can be answered from our work in which we had additionally applied this method to analyze the changes in MS lesions' shape and size overtime [18,19]. In that study, the changes in size and shape of 10 individual MS lesions were analyzed over 24 time points acquired during a 1-year period. The results demonstrated that most of the studied lesions undergo notable geometrical changes over time. Those changes were not necessarily associated with similar changes in size/volume. Furthermore, it was found that the I_l indices corresponding to changes in lesion shape could be 1.4 to 8.0 times higher than those corresponding to changes in the lesion size/volume.

In conclusion, the use of a set of analytical I_l indices, obtained from the SH together with the MDTV parameter, is an adequate method for analyzing the changes in MS lesions' shape and size. The selection of the value of n used to reconstruct the 3D surfaces could have a large impact on the MDTV value especially if a high n value is selected and the 3D surface get distorted. In order to prevent a large impact on the MDTV value, the n value shall be selected as referred above (see section "Characterization of lesion geometry using spherical harmonics"). Although the current results could be seen as a modest improvement in the variability of the measurement, it should be remarked that this is an analytically based approach giving at least the same results as other physical or computational methods, which are by far more complicated to implement and more time consuming. As compared with the CA method regarding the time and work that is involved in analyzing MS lesions with our approach, both techniques require the previous segmentation of the lesions from the MR images, and then it only takes a few seconds per each position on a PC Pentium II 399 MHz. We believe that the proposed analysis should improve if sets of MR images would have a better in-plane (i.e., voxel size) and through-plane (i.e., slice thickness) resolution. Moreover, if the approach is used together with a good repositioning technique, or after the implementation of automated image registration and segmentation algorithms [20], the obtained results can probably be further improved. This combination of techniques can be useful in reducing at least part of the errors that affect the analysis of changes of MS lesions during follow-up studies.

Acknowledgments

We thank Prof. Jacob Rubinstein and Oleg Michaelovich for their useful advice. The financial support of The "Sociedad Venezolana Amigos del Technion" (D.G.Z) is gratefully acknowledged. This investigation was supported in part by NIH grants P41 RR13218, R21 MH67054, R01 LM007861, P01 CA67165, and a research grant from the Whitaker Foundation. We express our deep gratitude to the people of the National Research Specimen Bank. The Multiple Sclerosis Human Neurospecimen Bank, Los Angeles CA, for providing us the in vitro brains with exceptional attention, as well as to Mrs. Rachel Moscovitz from the MRI Unit, Sheba Medical Center, Tel Hashomer, for her outstanding technical assistance.

References

[1] Barkhof F, Filippi M, Miller DH, Tofts P, Kappos L, Thompson AJ. Strategies for optimizing MRI techniques aimed at monitoring disease activity in multiple sclerosis treatment trials. J Neurol 1997;244:76–84.

[2] Badran AK, Durrani TS, Fisher AC, Paul JP. Patient realignment in magnetic resonance imaging of the head: an algorithm using mathematical morphology for feature extraction. J Biomed Eng 1990;12:138–42.

[3] Hajnal JV, Saeed N, Oatridge A, Williams EJ, Young IR, Bydder GM. Detection of subtle brain changes using subvoxel registration and subtraction of serial MR images. J Comput Assist Tomogr 1995;19:677–91.

[4] Wiebe S, Lee DH, Karlik SJ, et al. Serial cranial and spinal cord magnetic resonance imaging in multiple sclerosis. Ann Neurol 1992;32:643–50.

[5] Stone LA, Albert PS, Smith ME, et al. Changes in the amount of diseased white matter over time in patients with relapsing-remitting multiple sclerosis. Neurology 1995;45:1808–14.

[6] Filippi M, Marciano N, Capra R, et al. The effect of imprecise repositioning on lesion volume measurement in patients with multiple sclerosis. Neurology 1997;49:274–6.

[7] Guttmann CRG, Kikinis R, Anderson MC, et al. Quantitative follow-up of patients with multiple sclerosis using MRI: reproducibility. J Magn Reson Imaging 1999;9:509–18.

[8] Max NL, Getzoff ED. Spherical harmonics molecular surfaces. IEEE Comput Graph Appl 1988;8:42–50.

[9] Goldberg-Zimring D, Azhari H, Miron S, Achiron A. 3-D surface reconstruction of multiple sclerosis lesions using spherical harmonics. Magn Reson Med 2001;46:756–66.
[10] Jackson JD. Classical electrodynamics. New York: John Wiley & Sons, 1999.
[11] Akima H. A new method of interpolating and smooth curve fitting based on local procedures. Assoc Comput Mach 1970;17:589–602.
[12] Goldberg-Zimring D, Achiron A, Miron S, Faibel M, Azhari H. Automated detection and characterization of multiple sclerosis lesions in brain MR images. Magn Reson Imaging 1998;16:311–8.
[13] Mallat S. A wavelet tour of signal processing. New York: Academic Press, 1999.
[14] Rovaris M, Gawne-Cain ML, Sormani MP, Miller DH, Filippi M. The effect of repositioning on brain MRI lesion load assessment in multiple sclerosis: reliability of subjective quality criteria. J Neurol 1998;245:273–5.
[15] Firbank MJ, Coulthard A, Harrison RM, Williams ED. Partial volume effects in MRI studies of multiple sclerosis. Magn Reson Imaging 1999;17:593–601.
[16] Gawne-Cain ML, Webb S, Tofts P, Miller DH. Lesion volume measurement in multiple sclerosis: how important is accurate repositioning? J Magn Reson Imaging 1996;6:705–13.
[17] Mugler JP, Bao S, Mulkern RV, et al. Optimized single-slab three-dimensional spin-echo MR imaging of the brain. Radiology 2000; 216:891–9.
[18] Goldberg-Zimring D, Achiron A, Guttmann CRG, Azhari H. 3-D Analysis of individual multiple sclerosis lesions' geometry: detection of shape changes over time using spherical harmonics. J Magn Reson Imaging 2003;18:291–301.
[19] Goldberg-Zimring D, Achiron A, Guttmann CRG, Azhari H. Analysis of individual changes of multiple sclerosis lesions' 3-D geometry over time using spherical harmonics. In: Book of abstracts: ISMRM 10th Scientific Meeting. Honolulu, HI;2002. p. 1197.
[20] Warfield S, Dengler J, Zaers J, et al. Automatic identification of gray matter structures from MRI to improve the segmentation of white matter lesions. J Image Guid Surg 1995;1:326–38.